Journal of Neurochemistry

JOURNAL OF NEUROCHEMISTRY | 2009 | 110 | 1107–1119 doi: 10.1111/j.1471-4159.2009.06208.x

The muscarinic M1 receptor activates Nrf2 through a signaling cascade that involves protein kinase C and inhibition of GSK-3beta: connecting neurotransmission with neuroprotection

Sandra Espada, Ana I. Rojo, Marta Salinas and Antonio Cuadrado

Centro de Investigación Biomédica en Red sobre Enfermedades Neurodegenerativas (CIBERNED), Instituto de Investigaciones Biomédicas "Alberto Sols" UAM-CSIC, and Departamento de Bioquímica, Facultad de Medicina, Universidad Autónoma de Madrid, Madrid, Spain

Abstract

In this study, we provide evidence that the muscarinic M1 receptor targets NF-E2-related factor-2 (Nrf2), a transcription factor that regulates the expression of genes containing antioxidant response elements (AREs) in their promoters and that collectively constitute the phase II antioxidant response. In hippocampal primary and cerebellar granule neuron cultures expressing endogenous M1 receptor, carbachol increased the levels of a prototypical phase II antioxidant enzyme, heme oxygenase-1. Moreover, in a heterologous system, based on lentiviral expression of M1 receptor in PC12 pheochromocytoma cells, we found that M1 increased total and nuclear Nrf2 protein levels and heme oxygenase-1 messenger RNA and protein levels. Luciferase reporter constructs for AREs and the use of two inhibitors of protein kinase C (PKC), chelerythrine and 2-aminoethyl diphenylborinate, or transfection with relevant expression vectors allowed us to identify Gαq, phospholipase C-β and the classical PKC-γ isoenzyme, as responsible for the regulation of Nrf2. A PKC-insensitive Nrf2S40A single-point mutant partially channeled M1 signaling to AREs, therefore suggesting the participation of additional intermediates. Inhibition of glycogen synthase kinase-3β (GSK-3β) augmented M1-dependent activation of AREs while a PKC-insensitive mutant of GSK-3β (GSK-3β-Δ9) blocked this effect and prevented M1-induced accumulation of Nrf2 in the nucleus. Our results demonstrate a previously unidentified role of the Gαq/phospholipase C-β/PKC/GSK-3β axis in regulation of Nrf2 by M1. Such role provides additional conceptual support for the use of cholinemimetics in the treatment of pathologies that, like Alzheimer's disease, require a reinforcement of the cell antioxidant capacity.

Keywords: oxidative stress, acetylcholine, heme oxygenase, NF-E2-related factor-2.

J. Neurochem. (2009) **110**, 1107–1119.

Nerve cells are submitted to an oxidant environment that results from their aerobic metabolism, exposure to endogenous and exogenous neurotoxins and neuroinflammatory reactions (Moreira *et al.* 2005; Butterfield *et al.* 2006). To limit the abundance of reactive oxygen species (ROS) aerobic cells, including nerve cells, have developed an antioxidant response that tunes balance between ROS production and destruction.

Key to control of redox homeostasis is (NF-E2-related factor-2) Nrf2. It is a basic leucine-zipper transcription factor that binds antioxidant response elements (AREs) located at the promoters of antioxidant and drug-metabolizing genes (Kensler *et al.* 2007). These genes code for heme oxygenase-1 (HO-1), NAD(P)H: quinone oxidoreductase 1, glutathione *S*-transferases, glutamate-cysteine ligase, glutathione peroxidases, etc. (Kobayashi *et al.* 2004; Katoh *et al.* 2005). Taken together, these genes represent a cytoprotective reaction against multiple insults and constitute the so-called phase II response.

NF-E2-related factor-2 (Nrf2) is regulated at the level of protein stability, dimmer formation with bZip members of the

Received October 16, 2008; revised manuscript received May 9, 2009; accepted June 1, 2009.

Address correspondence and reprint requests to Dr Antonio Cuadrado, Departamento de Bioquímica, Facultad de Medicina, UAM, C/Arzobispo Morcillo 4, 28029 Madrid, Spain. E-mail: antonio.cuadrado@uam.es

Abbreviations used: 2-APB, 2-aminoethyl diphenylborinate; AREs, antioxidant response elements; Cch, carbachol; GSK-3, glycogen synthase kinase-3; HO-1, heme oxygenase-1; LUC, luciferase; Nrf2, NF-E2-related factor-2; PBS, phosphate-buffered saline; PKC, protein kinase C; PLC, phospholipase C; ROS, reactive oxygen species; SDS, sodium dodecyl sulfate.

Jun and Maf families, and subcellular localization (Kobayashi and Yamamoto 2005; Tong *et al.* 2006; Zhang 2006). In the absence of oxidant injury Nrf2 interacts with the BTB-Kelch protein Keap1, and this association promotes Nrf2 degradation through the ubiquitin-proteasome pathway. On the other hand, electrophiles promote the alteration of Nrf2-Keap1 complexes resulting in stabilization of the Nrf2 protein, and translocation to the nucleus, where it induces transcription of phase II genes (Tong *et al.* 2006). Preliminary evidences suggest that down-regulation of Nrf2 transcriptional activity is dependent on its redistribution back to the cytosol and degradation. In this regard, we have reported that glycogen synthase kinase-3β (GSK-3β), a kinase strongly implicated in the pathogenesis of Alzheimer's and other neurologic diseases, inhibits Nrf2 activity and the phase II response by excluding Nrf2 from the nucleus (Salazar *et al.* 2006; Rojo *et al.* 2008a,b).

Therefore, a fairly comprehensive knowledge is being generated on the mechanistic regulation of Nrf2 and its target genes. However, a complete picture is lacking on how this transcription factor is regulated in response to physiological signals such as those elicited by growth factors and neurotrophins. What is more important to this study, very little is known about the regulation of Nrf2 by neurotransmitter receptors, which should be quantitatively the most relevant in nerve cells.

Ectopic expression of genes encoding a single muscarinic receptor subtype in mammalian cell lines has provided an important model system in which to investigate receptor subtype-specific signal transduction (Felder 1995). Five subtypes (M1 to M5) have so far been identified, M1 being abundant in brain, including hippocampus (Levey *et al.* 1991; Wei *et al.* 1994; Wess 2003). M1 couples Gαq-proteins to activate phosphatidylinositol hydrolysis and the subsequent mobilization of calcium and activation of protein kinase C (PKC) isoenzymes (Felder 1995). PKC-γ, which is abundant in hippocampus and co-localizes with neurons expressing the M1 receptor may be particularly relevant to M1 signaling (Delmas *et al.* 2002; Rossi *et al.* 2005).

Muscarinic acetylcholine receptors have been implicated in neural plasticity (Jerusalinsky *et al.* 1997) and in several disorders such as Alzheimer's disease (Caccamo *et al.* 2006) (Fisher *et al.* 2002a; Fisher *et al.* 2002b; Fisher *et al.* 2003; Koch *et al.* 2005; Youdim and Buccafusco 2005; Felder *et al.* 2000). For this reason, several strategies have aimed at maintaining a basal threshold of acetylcholine stimulation through the use of either acetylcholinesterase inhibitors or acetylcholine agonists. The muscarinic M1 receptor is the most abundant subtype in cortex and hippocampus and has been the object of research for restoring cholinergic function. For instance, La Ferla's group has reported that in transgenic mice expressing human mutant APP and tau, both amyloid deposition and tau pathologies were reduced in the hippocampus and cortex when these animals were treated with a M1 agonist (Caccamo *et al.* 2006). However, the potential role of M1 activation in protection against oxidative stress has not been addressed despite the fact that ROS production may be tightly connected to the etiopathology of this and other neurodegenerative diseases with cholinergic dysfunction.

By using ectopic expression of the muscarinic M1 receptor in PC12 cells, in this study we have explored the role of M1 receptor-activation in regulation of the antioxidant cell response. We have also dissected the signaling pathway leading to activation of Nrf2-responsive genes taking HO-1 as a reference. In addition to the previously reported activation of Nrf2 by PKC, our results demonstrate a new role of the PKC/GSK-3β axis in regulation of Nrf2 by the metabotropic M1 receptor. This study identifies an additional therapeutic benefit of M1 agonists because of the reinforcement of the cell antioxidant capacity.

Experimental procedures

Cell culture and reagents

Rat pheochromocytoma PC12 cells were grown in Dulbecco's modified Eagle's medium supplemented with 7.5% heat-inactivated fetal bovine serum, 7.5% heat-inactivated horse serum and 80 μg/mL gentamicin (Salinas *et al.* 2003). Hippocampal primary cultures were prepared from Sprague–Dawley rats at embryonic day 18. Cells were seeded on poly-D-lysine-coated culture dishes and maintained in Dulbecco's modified Eagle's medium supplemented with 10% horse serum for 2 h. Then, the cultures were shifted to neurobasal medium supplemented with B27-minus antioxidants (Invitrogen, Madrid, Spain), 2 mM glutamine, 100 μg/mL streptomycin and 100 U/mL penicillin. On day 3, cells were treated for 24 h with 10 μM 1-(β-D-arabinofuranosyl)cytosine (Sigma, Madrid, Spain) to reduce the number of proliferating non-neuronal cells. Neurons were used at day 10. Primary cultures of cerebellar granule neurons were prepared from 8-day-old Sprague–Dawley rats. Cerebella were dissected, stripped of meninges, and incubated at 37°C for 15 min with trypsin solution (1% trypsin diluted in Hank's balanced salt solution, 1.2 mmol/L $MgCl_2$, 3% bovine serum albumin and 50 U/mL of deoxyribonuclease I; all reagents from Sigma). Then, a trypsin-stop solution (0.720 mmol/L $MgCl_2$, 20% fetal bovine serum and 40 U/mL of deoxyribonuclease I diluted in Hank's balanced salt solution) was added and samples were centrifuged at 200 *g* for 5 min. Pelleted cells were re-suspended in the same solution and mechanically dissociated with a fire-polished Pasteur pipette. Cells were collected by centrifugation at 200 *g* for 10 min and seeded on poly-D-lysine-coated culture dishes. Culture medium was neurobasal-B27 medium (B27-minus antioxidants), containing 25 mmol/L KCl, 1 mmol/L glutamine, and antibiotic, 80 mg/mL gentamicin. 1-(β-D-arabinofuranosyl)cytosine (10 μmol/L) was added to avoid the proliferation of glial cells. Neurons were used at day 10. Carbachol (Cch) was purchased from Calbiochem (Nottingham, UK). SB216763, chelerythrine and 2-aminoethyl diphenylborinate (2-APB) were purchased from Sigma-Aldrich.

Plasmids

Transient transfections of PC12 cells were performed with the expression vectors pcDNA 3.1, pGL3-basic (Promega, Madrid, Spain), pHO1-15-luciferase (LUC), ARE-LUC, pEFΔNrf2-DN (gift of Dr J. Alam, Department of Molecular Genetics, Ochsner Medical Center, New Orleans, LA, USA), pCEFL, pCEFL-Gβ1, pCEFL-Cγ2, pCEFL-M1, pcDNA3.1-GαqQ209L (gifts of Dr S. Gutkind, Oral and Pharyngeal Branch, National Institute of Dental and Cranio-Facial Research, NIH, Bethesda, MD, USA), pMV7gpt-phospholipase C (PLC)-β, pMT2-PKC-I (Cuadrado *et al.* 1990), pcDNA3.1.V5HisBmNrf2 (gift of Dr D.J. Hayes, Biomedical Research Centre, Ninewells Hospital and Medical School, University of Dundee, Dundee, UK), pcDNA3.1Gαq-Ct (Arai *et al.* 2003), pCGN-HA-GSK3β-(Y216F) and pCGN-GSK3β-Δ9 (gift of Dr A. Kikuchi, Department of Biochemistry, Faculty of Medicine, Hiroshima University). pcDNA3.1V5HisBmNrf2S40A was generated with the Gene Tailor site-directed mutagenesis kit according to manufacturer's instructions (Invitrogen) using the primers forward 5′-GTCGAGAAGTGTTTGACTTTGCTCAGCGACAG-3′ and reverse, 5′-AAAGTCAAACACTTCTCGACTTACTC-CAAG-3′. For lentiviral production, we used the expression vectors psPAX2, pMD2G and pWPXL (Dr Trono Didier, School of Life Sciences, Ecole Polytechnique Fédérale de Lausanne, Switzerland). Plasmid pWPXL-M1 was generated in two steps: first, the green fluorescence protein coding sequence was replaced by an oligonucleotide cloned between the *Bam*HI and *Eco*RI sites of pWPXL (forward: 5′-CGCGTATTCGGTCACCGTAAG-3′ and reverse: 5′-AATTCTTACGGTGACCGAATA-3′); second, the *Eco*RI/*Not*I fragment from pCEFL-M1, containing the full coding sequence of the M1 receptor, was subcloned into the *Eco*RI/*Sma*I sites of this modified version of pWPXL (the *Not*I site of the insert was klenow filled to allow ligation at the *Sma*I site).

Luciferase assays

PC12 cells were seeded in 24-well plates (75 000 cells per well), cultured for 16 h, and transfected with a DNA mixture consisting of 300 ng of the appropriate LUC construct and effector/control plasmids up to 900–1200 ng of total DNA, using lipofectamine reagent (Invitrogen). Cells were incubated with DNA/lipofectamine complexes for 5 h, and then maintained in low-serum medium (0.25% fetal bovine serum, 0.25% horse serum) for 16 h. LUC activity was assayed with the LUC Assay System (Promega), according to the manufacturer's instructions, and relative light units were measured in a BG1 Optocomp I, GEM Biomedical luminometer (Optocomp Corp., Sparks, NV, USA). Values of LUC activity obtained with the ARE-LUC reporter were normalized with those of cells transfected in parallel with pGL3-basic (Promega) under the same conditions and are presented as fold of increase over control vector transfected or untreated cells. LUC experiments were performed at least three times using 3–4 samples per group. A Student's *t*-test was used to assess differences between groups ($p < 0.05$). The values in graphs correspond to the mean ± SD.

Lentivirus production

Packaging of the lentiviral expression vector described above, pWPXL-m1, was produced by calcium-phosphate transfection in HEK293T cells. 33×10^6 of HEK293T cells were distributed in three 150 cm culture plates and were transfected 1 day later with the expression vectors pMD2G, pSPAX2, and pWPXL-M1. Lentiviruses were collected from cell culture medium after 48 h and concentrated through Millipore Centricon Plus-20 100 K (Billerica, MA, USA). Final titters were in the range of 10^6 infective particles/mL.

Preparation of nuclear extracts

PC12M1 cells were transiently transfected with Lipofectamin 2000 reagent using pcDNA3.1.V5HisBmNrf2 or pCGN-HA-GSK3β-(Y216F) or pCGN-HA-GSK3β-(Δ9) plasmids. Nuclear and cytosolic fractions were prepared as previously described (Rojo *et al.* 2004). Briefly, 2×10^6 cells were washed three times with cold phosphate-buffered saline (PBS) and harvested by centrifugation. The cell pellet was re-suspended in three pellet volumes of cold buffer A [containing in mM: 20 HEPES, pH 7.0, 0.15 EDTA, 0.015 EGTA, 10 KCl, 1 phenylmethylsulfonyl fluoride, 20 NaF, 1 sodium pyrophosphate, and 1 Na_3VO_4 plus 1% Nonidet P-40 (Sigma, Madrid, Spain), 1 μg/mL leupeptin]. Then, the homogenate was centrifuged at 500 *g* for 5 min. Supernatants, corresponding to cytosolic fractions, and the nuclear pellets were re-suspended in five pellet volumes of cold buffer B (containing in mM: 10 HEPES, pH 8.0, 0.1 EDTA, 1 phenylmethylsulfonyl fluoride, 20 NaF, 1 sodium pyrophosphate, and 1 Na_3VO_4 plus 25% glycerol, 0.1 M NaCl, 1 μg/mL leupeptin). After centrifugation in the same conditions indicated above, the nuclei were resuspended in 2% sodium dodecyl sulfate (SDS) containing buffer. Cytosolic and nuclear fractions were resolved in SDS–polyacrylamide gel electrophoresis and immunoblotted with the indicated antibodies.

Immunoblotting and densitometry

Cells were washed once with cold PBS and lysed on ice with 200 μL of lysis buffer (1% Nonidet P-40, 10% glycerol, 337 mM NaCl, 20 mM Tris–HCl, pH 7.5, 1 μg/mL leupeptin, 1 mM phenylmethylsulfonyl fluoride, 20 mM NaF, 1 mM sodium pyrophosphate, and 1 mM Na_3VO_4). Lysates were pre-cleared by centrifugation, resolved by SDS–polyacrylamide gel electrophoresis, and transferred to Immobilon-P membranes (Millipore). Blots were analyzed with the appropriate primary antibodies (1 : 1000). The antibodies used were: anti-HO-1 from Millipore, anti-Nrf2 and β-actin from Santa Cruz Biotechnology (Heidelberg, Germany), anti-phospho-GSK-3β(Ser9) from Cell Signalling (Boston, MA, USA), and anti-GSK-3β from BD Biosciences (Madrid, Spain). Peroxidase-conjugated secondary antibodies (1 : 10 000) were used to detect the proteins of interest by enhanced chemiluminescence. Protein bands were scanned and density was analyzed with the MCID Image Analysis software (InterFocus Imaging Ltd, Cambridge, UK). Densitometric values were obtained for three samples of each experimental condition.

Northern blots

Total RNA was isolated from PC12 and PC12M1 cells using Trizol reagent (Invitrogen). The amount of total RNA obtained was determined by spectrophotometry at 260 nm. Twenty micrograms of total denatured RNA were run in 1% agarose-2.2 M formaldehyde gels and blotted onto nitrocellulose membranes. A 200 bp fragment of rat HO-1 cDNA was labeled to a specific activity of 10^9 cpm/ng with [^{32}P]-ATP (2000 Ci/mmol; Amersham International, London,

UK) following standard procedures and was used for hybridization at a concentration of 10 ng/mL.

[^{3}H]-Scopolamine binding

Experiments were performed in 24-well plates. PC12 and PC12M1 cells were seeded at a density of 50 000 cells per well and grown for 48 h. [^{3}H]-scopolamine binding was determined in cells incubated with 3 nM 1-[*N*-methyl-^{3}H] scopolamine methyl chloride (81 Ci/mmol; Amersham International) for 2 h at 4°C. Non-specific binding was estimated in parallel samples from cells incubated with 3 nM [^{3}H]-scopolamine plus 300 nM cold scopolamine. Specific binding was displaced by pre-incubating the cells with 10 μM atropine for 15 min before starting the scopolamine binding assay. Binding reactions were terminated by washing three times with ice-cold medium. [^{3}H]-scopolamine was extracted by solubilizing the cells with 500 mL 0.5 M NaOH for 1 h and the amount of bound [^{3}H]-scopolamine was correlated to the number of cells in replica plates.

Immunocytochemistry

Cells were seeded in 24-well plates (75 000 cells per well), on poly-D-Lysine covered slides, cultured for 16 h and infected with 10 infective particles/cell of lentiviral pWPXL-M1 vector. After 2 days cells were washed with cold PBS and fixed by incubation for 15 min at 22°C with 4% paraformaldehyde. Then, cells were washed three times with PBS and permeabilized with 0.25% Nonidet P-40 for 10 min. The slides were incubated with anti-M1 receptor antibody (1 : 100) (Millipore) for 1.5 h at 37°C in a humidified chamber. Then, cells were washed three times with PBS and incubated with Alexa Fluor 488-conjugated antibody (1 : 200) (Invitrogen) for 45 min under the same conditions. To visualize the nuclei, cells were stained during the last wash with 4′,6-diamidino-2-phenylindole. The fluorescence images were captured using a Zeiss Axiophot system (Zeiss, Madrid, Spain) with standard excitation filters of BP 450/90 nm (Alexa) and 365/12 nm (4′,6-diamidino-2-phenylindole).

Results

Acetylcholine-agonists induce HO-1 expression in primary neuronal cultures that express the M1 receptor

We analyzed the effect of the acetylcholine agonist Cch on the expression of the antioxidant enzyme HO-1 in rat primary hippocampal cells. As shown in Fig. 1(a and c), these neurons expressed the acetylcholine receptor M1 and, following 6 h incubation with 1 mM Cch, they exhibited a threefold increase in HO-1 protein levels. Similar results were obtained in cerebellar primary neurons (Fig. 1b and c). Then, we compared the effect of Cch with a different acetylcholine agonist, pilocarpine, and with the antagonist dicyclomine in cerebellar granule neurons (Fig. 1c). Both Cch and pilocarpine induced about threefold increase of HO-1 levels but co-incubation with dicyclomine drastically reduced HO-1 induction. Additional evidence on HO-1 induction by Cch was obtained by immunofluorescence of hippocampal primary neurons submitted to Cch for 16 h (Fig. 1e). As Cch-mediated induction of HO-1 expression

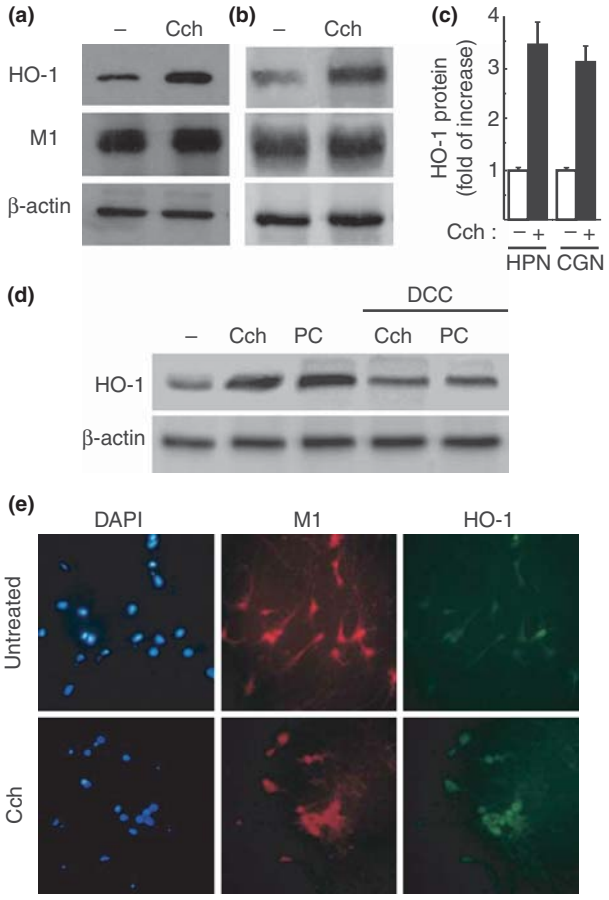

Fig. 1 Acetylcholine agonists increase HO-1 protein levels in rat primary neurons expressing the muscarinic M1 receptor. (a and b) Immunoblots from primary hippocampal neurons (a) and cerebellar granule neurons (b) incubated for 6 h with 1 mM Cch. Upper panels, anti-HO-1 antibody; middle panels, anti-M1 receptor antibody; lower panels, anti-β-actin antibody. (c) Densitometric analysis of three similar experiments showing HO-1 protein increase in hippocampal neurons (HPN) and cerebellar granule neurons (CGN) after 6 h in Cch. HO-1 protein levels were normalized with β-actin. (d) Immunoblots from cerebellar granule neurons incubated for 6 h with Cch (1 mM), pilocarpine (PC, 1 mM) and dicyclomine (DCC, 10 μM) as indicated. Upper panels, anti-HO-1 antibody; middle panels, anti-M1 receptor antibody; lower panels, anti-β-actin antibody. (e) Immunofluorescence analysis of M1 and HO-1 protein in hippocampal primary neurons submitted to Cch for 6 h. Blue, DAPI-stained nuclei; red, anti-M1 antibody; green, anti-HO-1 antibody. Arrows point cells that do not express M1 and do not increase HO-1 staining in response to Cch.

took place in neurons expressing the muscarinic M1 receptor, in this study we analyzed the possibility that M1 might activate a signaling pathway leading to induction of the antioxidant cell response.

Over-expression of functional M1 receptor in PC12 cells

PC12 cells expressing M1 receptor (from now on PC12M1 cells) were generated by infection with a lentiviral expression

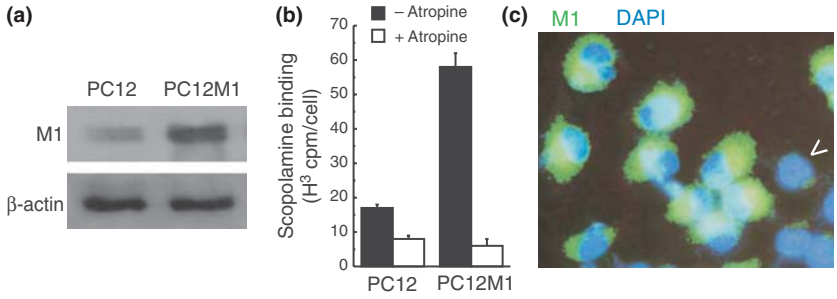

Fig. 2 Over-expression of M1 receptor in PC12 cells. (a) Immunoblot showing M1 receptor protein in control PC12 and PC12M1 cells. Upper panel, anti-M1 receptor antibody; lower panel, anti-β-actin antibody. Densitometric analysis of three similar experiments indicating an increase of 6.2 ± 0.4 SD in M1 receptor protein levels after normalization with β-actin. (b) Comparison of high affinity binding sites for the muscarinic agonist scopolamine in PC12 and PC12M1 cells (see 'Experimental procedures' for details). Each value is the mean of six samples ± SD. (c) Immunofluorescence of PC12M1 cells stained with anti-M1 antibody (green) and counter-stained with DAPI (blue). The arrow points a cell that was not stained with the M1 antibody, therefore providing a negative control for background staining.

vector for M1 (pWPXL-M1). As shown in Fig. 2(a), M1 receptor was barely detectable in PC12 cells. However, 48 h after pWPXL-M1 lentiviral infection we observed a 6.2-fold increase in M1 immunoreactivity. Moreover, analysis of high affinity binding sites with the muscarinic agonist [^{3}H]-scopolamine (3 nM) indicated over fourfold increase in the number of high affinity binding sites that were competed out by pre-incubation for 15 min with a 100-fold excess of non-radioactive scopolamine or with the muscarinic antagonist atropine (Fig. 2b). Over 85% of PC12M1 cells, generated by infection with lentiviral pWPXL-M1 expression vector (10 infective particles per cell) were stained by the M1 receptor antibody (Fig. 2c). Control PC12 cells, infected with empty lentiviral vector (pWPXL), were not stained with a M1 receptor antibody (data not shown).

Activation of M1 muscarinic receptor results in up-regulated HO-1 gene expression

Control PC12 and PC12M1 cells were maintained in low-serum medium for 16 h and then they were treated with the strong HO-1 inducer hemin (50 μM) or several Cch concentrations ranging from 0.03 to 1 mM for 6 h as indicated in Fig. 3(a and b). Control PC12 cells exhibited increased HO-1 protein levels in response to hemin but were almost unresponsive to Cch (up to 1.5-fold increase over basal non-stimulated cells), suggesting that endogenous cholinergic receptors either do not induce HO-1 expression or their abundance is too low to elicit a significant response. On the contrary, PC12M1 cells exhibited a significant increase in HO-1 protein levels following 6 h treatment with Cch and reached maximal induction at concentrations over 0.1 mM. As there were not any signs of toxicity at the Cch concentrations used, a dose of 1 mM was chosen for the following experiments to ensure an optimal response.

We determined messenger RNA levels in response to Cch. As shown in Fig. 3(c), HO-1 mRNA levels did not significantly change in control PC12 cells. By contrast, in PC12M1 cells HO-1 mRNA was elevated at 4 and 6 h after Cch treatment. Also, we analyzed the effect of M1 activation on HO-1 expression using a LUC reporter construct that carries the LUC gene under the control of 15 Kb from the 5′-promoter region of the mouse *hmox1* gene (pHO1-15LUC) and the promoterless pGL3-basic vector as a control. PC12 cells were co-transfected with pHO1-15LUC and a M1 expression vector (pCEFL-M1). After transfection, cells were maintained in low-serum medium for 16 h in the presence or absence of Cch. As shown in Fig. 3(d), PC12 cells transfected with empty vector did not significantly induce the HO-1 promoter. By contrast, Cch elicited an M1-dependent up-regulation of this promoter. Taken together these results indicate that Cch uses the M1 receptor to induce HO-1 expression.

Induction of HO-1 by the M1 receptor is dependent on Nrf2 transcriptional activity

Because Nrf2 is crucial to regulation of cell redox homeostasis, we sought to analyze if M1 might be targeting this transcription factor. Nrf2 activity was blocked by over-expressing its bZIP dimerization domain [ΔNrf2(DN)], which prevents heterodimerization of endogenous Nrf2. As shown in Fig. 4(a), M1 receptor activation of pHO1-15LUC reporter was substantially blocked in the presence of the dominant negative ΔNrf2(DN) mutant. As Nrf2 targets AREs, we analyzed if M1 might be inducing a signaling pathway involved in regulation of this enhancer in the *hmox1* gene, by using a LUC reporter containing three tandem sequences of the mouse *hmox1* ARE (ARE-LUC). PC12 cells were co-transfected with ARE-LUC and several amounts of M1 expression vector as indicated in Fig. 4(b). After transfection cells were placed in low-serum medium in the presence or absence of 1 mM Cch for 16 h. As shown in Fig. 4(b), Cch activated the ARE-LUC reporter in cells expressing M1.

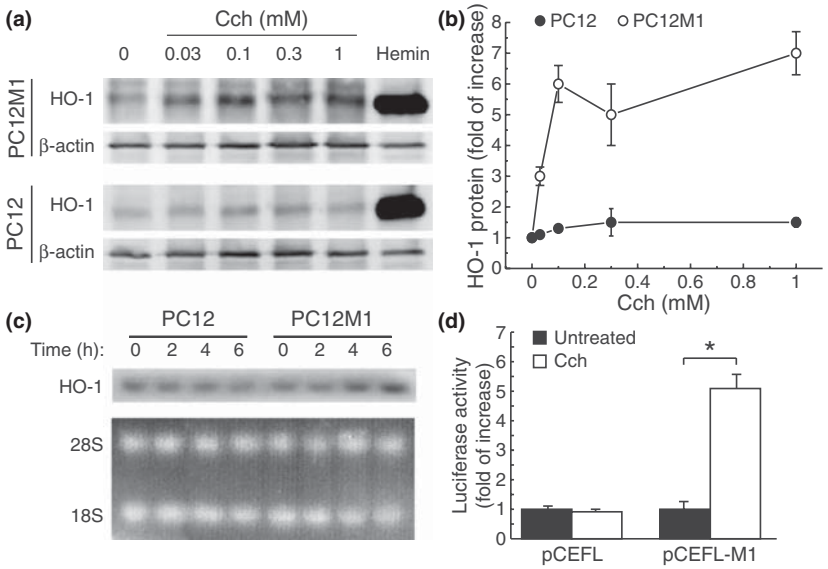

Fig. 3 Muscarinic receptor M1 induces HO-1 expression. (a) HO-1 protein levels in control PC12 and PC12M1 cells submitted to the indicated Cch concentrations or to 50 μM hemin for 6 h. Upper panels, immunoblots with anti-HO-1 antibody. Lower panels, immunoblots with anti-β-actin antibody showing similar amount of protein lysate per lane. (b) Densitometric quantification of (a). Each point is the average of three samples ± SD. (c) Northern blot analysis of HO-1 mRNA levels in PC12 and PC12M1 cells submitted to 1 mM Cch for the indicated times. Upper panel, autoradiogram showing HO-1 mRNA; lower panel, ethidium bromide-stained gel used for blotting of the upper panel, showing similar amount of total RNA per lane. (d) Luciferase assays showing M1-dependent induction of *hmox1* expression. PC12 cells were transfected with pHO1-15-LUC (or pGL3-basic as a control) and either control (pCEFL) or M1 expressing (pCEFL-M1) vectors. After 5 h cells were transferred to low-serum medium and submitted to 1 mM Cch for 16 h. Luciferase experiments were performed at least three times using 3–4 samples per group. The values in graphs correspond to the mean ± SD. A Student's *t*-test was used to assess differences between groups. Asterisks denote statistically significant differences with $p < 0.05$.

To further demonstrate the regulation of Nrf2 by M1 in the absence of other elements that might be involved in ARE regulation, we used an expression vector for a fusion protein containing the DNA-binding domain of the yeast transcription factor Gal4 and Nrf2 (Gal4-Nrf2). PC12 cells were co-transfected with empty vector or expression vector for M1 plus Gal4-Nrf2 expression construct and the Gal4-LUC reporter plasmid as indicated in Fig. 4(c). Cells co-transfected with Gal4-LUC and Gal4-Nrf2 exhibited a very strong increase in LUC activity compared to that of cells co-transfected with Gal4-LUC and empty vector. Moreover, when M1-expressing PC12 cells were co-transfected with the same plasmids and stimulated with Cch, we observed a significant three- to fourfold increase in LUC activity.

Next, we analyzed Nrf2 protein levels following M1 receptor activation. PC12M1 cells were maintained in low-serum medium for 16 h and then stimulated with 1 mM Cch. As shown in Fig. 4(d and e), Cch elicited a modest time-dependent increase in Nrf2 protein levels that was maximal between 3 and 6 h suggesting that M1 activation may lead to stabilization of this factor. Moreover, as shown in Fig. 4(f), Cch induced the nuclear accumulation of Nrf2 within 15–30 min. Taken together these results indicate that Nrf2 is targeted by the M1 receptor to activate AREs.

The muscarinic M1 receptor uses Gαq to stimulate AREs

To dissect the signaling pathway that leads to activation of AREs we analyzed the effect of Cch on PC12 cells co-transfected with an expression vector for M1 receptor and the carboxiterminal region of Gαq which exerts a dominant negative function on this G protein (Arai *et al.* 2003). As shown in Fig. 5(a), Cch alone induced about fivefold expression of AREs in M1-transfected PC12 cells. By contrast, when these cells were co-transfected with Gαq-Ct, induction of AREs by Cch was severely reduced. In additional experiments, we analyzed the effect of active GαqQ209L mutant. This single point mutant expresses a GTPase-deficient active subunit that elicits effector pathways in the absence of receptor stimulation (De Vivo *et al.* 1992; Neves *et al.* 2002). We also analyzed the effect of Gβ1 and Gβ1γ2 subunits which activate their own signaling pathways. LUC assays were conducted in PC12 cells co-transfected with ARE-LUC and expression vectors for these G subunits. As shown in Fig. 5(b), Gβ1 alone or in co-transfection with Gγ2 failed to activate AREs. On the contrary, GαqQ209L produced a potent ARE activation by

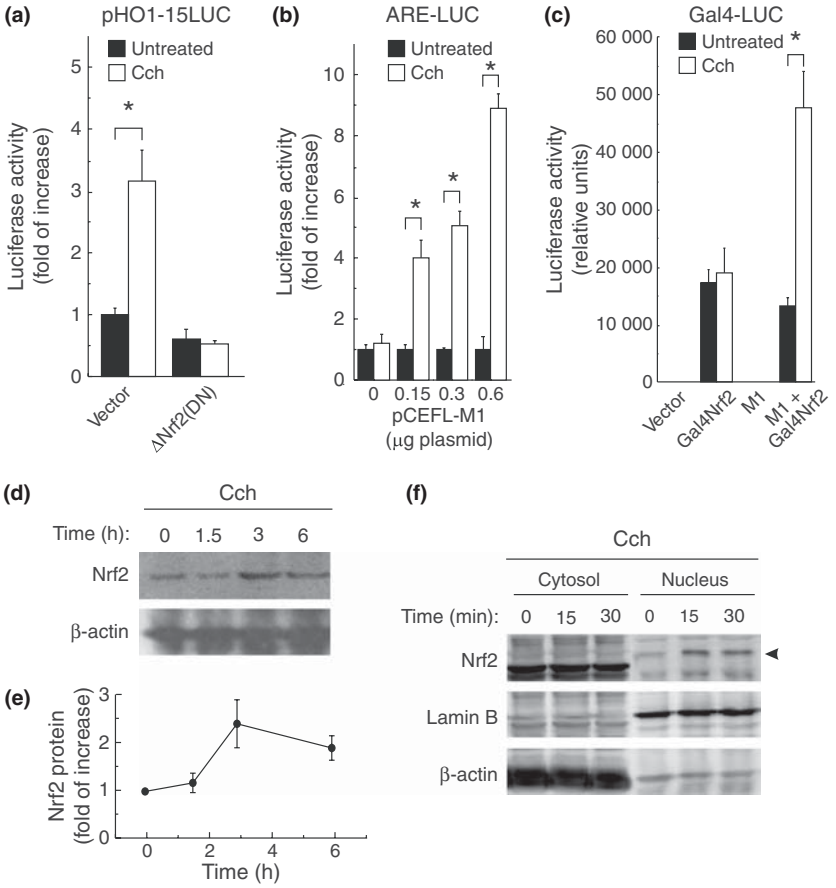

Fig. 4 M1 receptor targets Nrf2 to induce an antioxidant response. (a) M1 requires Nrf2 to activate the HO-1 promoter. PC12 cells were co-transfected with M1 expression vector (pCEFL-M1) and pHO1-15LUC (or pGL3-basic as a control) and either empty vector or dominant negative Nrf2 [ΔNrf2(DN)] expression vector. (b) M1 receptor activates AREs. PC12 cells were co-transfected with ARE-LUC (or pGL3-basic as a control) and increasing amounts of expression vector for M1 (pCEFL-M1). (c) M1 receptor uses the transactivating activity of Nrf2 to induce AREs. PC12 cells were co-transfected with Gal4-LUC (or pGL3-basic as a control) and either empty vector of expression vectors for Gal4Nrf2 and M1 as indicated. For (a–c), after transfection cells were placed in low-serum medium and submitted to 1 mM Cch for 16 h. Luciferase experiments were performed at least three times using 3–4 samples per group. The values in graphs correspond to the mean ± SD. A Student's *t*-test was used to assess differences between groups. Asterisks denote statistically significant differences with $p < 0.05$. (d and e) M1 receptor activation results in increased Nrf2 protein levels. PC12M1 cells were placed in low-serum medium for 16 h and then submitted to 1 mM Cch for the indicated times. (d) Upper panel, immunoblot with anti-Nrf2 antibody. Lower panel, immunoblot with anti β-actin antibody showing similar amount of protein lysate per lane. (e) Densitometric analysis of bands indicating small increases of Nrf2 protein levels at 3 and 6 h respectively. Nrf2 protein levels were normalized with those of β-actin. (f) Cch induces the nuclear translocation of Nrf2. PC12M1 cells were placed in low-serum medium for 16 h and then submitted to 1 mM Cch for the indicated times. Nuclear and cytosolic protein extracts were immunoblotted as indicated. Upper panel, anti-Nrv2 antibody. Middle panel, anti-lamin B antibody showing nuclear protein extracts. Lower panel, anti-β-actin antibody showing cytosolic protein extracts.

itself. These results indicate that Gαq is necessary and sufficient for M1 signaling to AREs.

Gαq signals to AREs through activation of PLC-β and PKC-γ

To analyze the pathway connecting Gαq with Nrf2 activation, first, we used the PKC inhibitor chelerythrine and the calcium blocker 2-APB to inhibit PKC signaling. Following transfection with ARE-LUC and either M1 or GαqQ209L expression vectors, cells were submitted for 16 h to Cch (1 mM) chelerythrine (0.5, 1, and 2 μM) or 2-APB (50, 100, and 200 μM) as indicated in Fig. 6(a and b). Both inhibitors, which have a different mechanism of action, dose-dependently blocked ARE activation by active M1 or by GαqQ209L. These experiments demonstrate a role of classical PKCs as mediators of AREs activation by the M1 receptor.

To determine the role of classical PKCs as mediators of the M1 response to AREs, we chose to analyze the PKC-γ isoform. Obviously other classical PKCs might be analyzed as well but this choice was based on observations that both

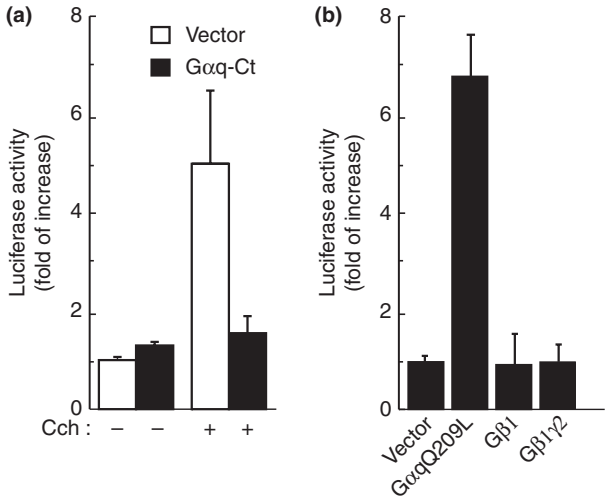

Fig. 5 The M1 receptor uses Gαq but not Gβγ to activate AREs. (a) Inhibition of Gαq signaling with dominant negative carboxiterminal mutant of Gαq (Gαq-Ct) impairs M1 signaling to AREs. Cells were co-transfected with M1 and Gαq-Ct and ARE-LUC (or pGL3-basic as a control). (b) Gαq but not Gβγ induces AREs. Cells were co-transfected with expression vectors for constitutively active Gαq(Q209L), Gβ1 and Gγ2 as indicated, together with ARE-LUC (or pGL3-basic as a control). Luciferase experiments were performed at least three times using 3–4 samples per group. The values in graphs correspond to the mean ± SD.

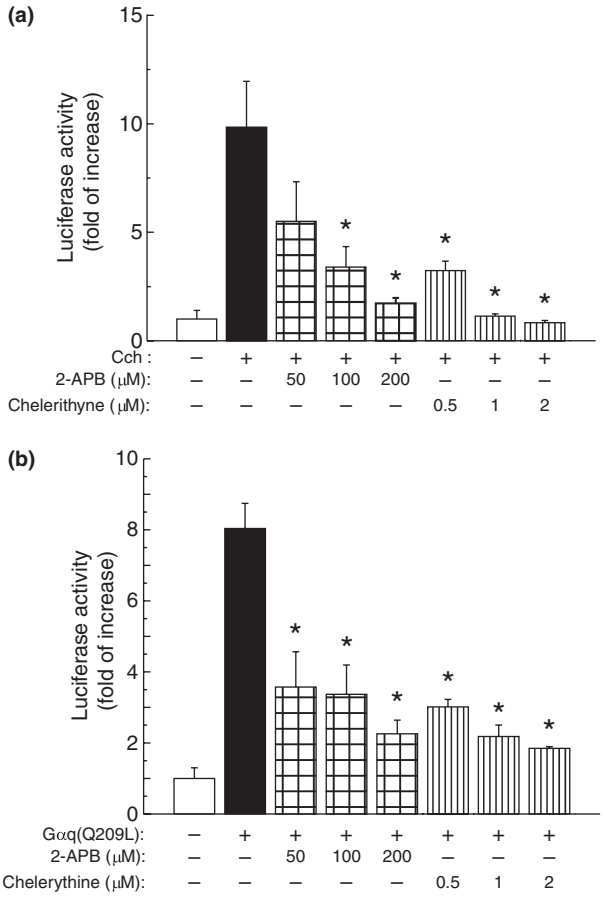

Fig. 6 The M1 receptor uses PKC to activate AREs. (a) Inhibition of PKC signaling prevents M1-mediated induction of AREs. PC12 cells were co-transfected with expression vector for M1 (pCEFL-M1) and ARE-LUC (or pGL3basic as control). (b) Inhibition of PKC signaling prevents Gαq(Q209L)-mediated induction of AREs. PC12 cells were co-transfected with expression vector for Gαq(Q209L) and ARE-LUC (or pGL3basic as control). After transfection, cells were placed in low-serum medium and treated with chelerythrine or 2-APB for 16 h. In (a), Cch was added 30 min after chelerythrine or 2-APB. Luciferase experiments were performed at least three times using 3-4 samples per group. A Student's *t*-test was used to assess differences between groups. The values in graphs correspond to the mean ± SD. Asterisks denote statistically significant differences with $p < 0.05$ between the untreated group and each of the chelerythrine- and 2-APB-treated groups.

M1 receptor and the PKC-γ isoform are abundant in hippocampus and co-localize in hippocampal neurons (unpublished data) (Rossi *et al.* 2005; Tang *et al.* 2004). We analyzed ARE-LUC activation in cells over-expressing active GαqQ209L and either PLC-β or PKC-γ or both. For these experiments we used an amount of Gαq expression vector lower than in Fig. 5(b) to avoid saturation (just twofold increase vs. the sevenfold increase of Fig. 5b). As shown in Fig. 7(a), PLC-β and PKC-γ cooperated with GαqQ209L to activate AREs, but the strongest induction was found when GαqQ209L, PLC-β, and PKC-γ were co-transfected together. Therefore, both pharmacological and genetic approaches provided strong evidence that the Gαq/PLC-β/PKC-γ axis leads to activation of AREs.

In view of the strong activation of ARE by this pathway and considering that Nrf2 is phosphorylated by several PKCs at Ser40 leading to its dissociation from Keap1 (Huang *et al.* 2002; Bloom and Jaiswal 2003), we investigated the regulation of Nrf2 by Gαq-mediated activation of PKC. PC12 cells were transfected with ARE-LUC and GαqQ209L expression vector plus increasing amounts of expression vector for Nrf2 or Nrf2S40A single point mutant (Fig. 7b). As expected, wild-type Nrf2 cooperated with GαqQ209L to induce ARE. On the other hand, the PKC insensitive mutant Nrf2S40A partially inhibited the Gαq-Q209L induction of ARE, particularly at low concentrations. Nevertheless, Nrf2S40A still cooperated with GαqQ209L to induce this enhancer. These results suggest that direct phosphorylation of Nrf2 by PKC at S40 participates in signaling from Gαq to Nrf2 but as Nrf2S40A still cooperated with GαqQ209L, other regulatory factors acting downstream from PKC must be involved as well.

Inhibition of GSK-3β mediates Nrf2 activation by the M1 receptor

Protein kinase C inhibits GSK-3β by phosphorylating its auto-inhibitory domain at Ser9. Therefore, we analyzed the putative role of GSK-3β in the regulation of Nrf2 by M1

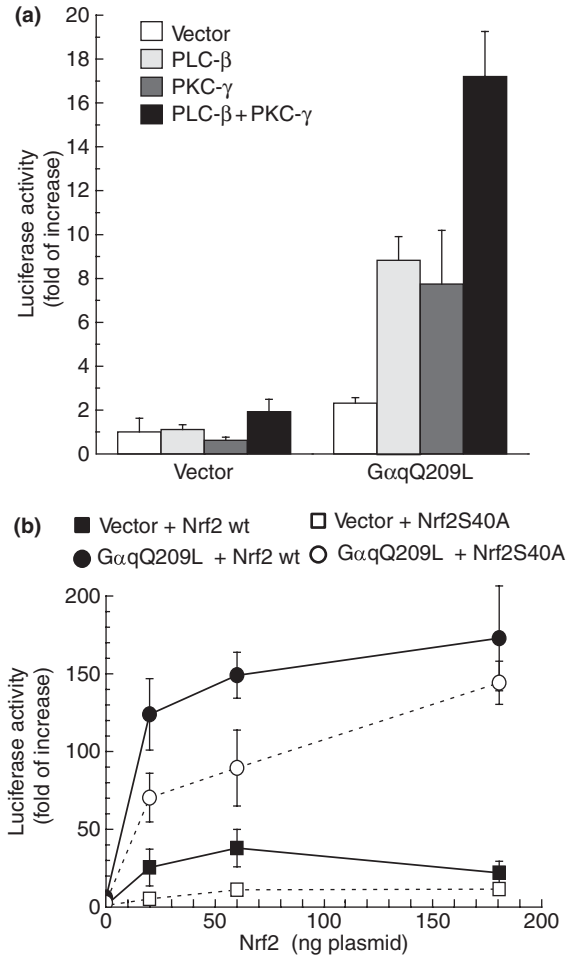

Fig. 7 Phospholipase C (PLC)-β and PKC-γ cooperate with Gαq to activate AREs. (a) PC12 cells were co-transfected with ARE-LUC (or pGL3-basic as a control) and either empty vector of expression vectors for the indicated proteins. (b) Ser40 of Nrf2 participates in the induction of AREs by the Gαq. PC12 cells were co-transfected with expression vector for GαqQ209L, ARE-LUC (or pGL3-basic as a control) and increasing amounts of Nrf2 wild type or Nrf2S40A single point mutant. After transfection, cells were placed in low-serum medium for 16 h and then analyzed for luciferase activity. Luciferase experiments were performed at least three times using 3-4 samples per group. Each value represents the mean of three samples ± SD.

receptors. PC12M1 cells were maintained in low-serum medium for 16 h and then stimulated with Cch for 10 min. Additionally, cells were pre-treated with chelerythrine for 30 min as indicated in Fig. 8(a). Cch induced the phosphorylation/inhibition of GSK-3β as determined with the phospho-Ser9-specific antibody. On the contrary, cells pre-treated with chelerythrine exhibited a much lower basal and Cch-induced phosphorylation of GSK-3β. We then analyzed the effect of the GSK-3β inhibition by SB216763 (a potent and selective cell permeable ATP-competitive inhibitor of GSK3 with an IC_{50} value of 34 nM) on the Cch-induced activation of AREs. As shown in Fig. 8(b), inhibition of GSK-3β was sufficient to activate this enhancer to values close to those of Cch alone. Moreover, the combined treatment with both SB216763 and Cch further increased ARE-Luc activation. Similar results were obtained with lithium (50 mM; EC_{50} 2 mM) (data not shown). These results suggest that a significant part of the effect of Cch on Nrf2 activation is mediated by GSK-3β.

To further confirm these results, we analyzed the subcellular distribution of Nrf2 in PC12M1 cells co-transfected with expression vectors for V5-tagged Nrf2 and either a control inactive HA-tagged single point mutant of GSK-3β (GSK-3β(Y216F)) or a constitutively active, HA-tagged deletion mutant GSK-3β which lacks the pseudosubstrate domain and is not regulated by PKC (GSK3β-Δ9). After transfection cells were maintained in low-serum medium for 24 h and then stimulated for 30 min with Cch. As shown in Fig. 8(c), ectopically expressed Nrf2-V5 was scarcely visible in the cytosol and nucleus of control cells. However, Cch induced a noticeable increase in nuclear Nrf2-V5 in agreement with data of Fig. 4(f) for the endogenous Nrf2. More importantly, expression of active GSK-3β-Δ9 partially blocked the Cch-induced nuclear translocation of Nrf2-V5. These results indicate that inhibition of GSK-3β by M1 signaling is required to elicit a full Nrf2 activation.

Finally, we analyzed the effect of GSK-3β-Δ9, which is not regulated by PKC, on the activation of AREs by Gαq. PC12 cells were transiently co-transfected with the LUC reporter ARE-LUC (or pGL3-basic as a control) and a fixed amount of either empty vector or GαqQ209L (0.6 μg/well). In addition, cells were also co-transfected with increasing amounts of GSK-3β-Δ9 expression vector as indicated in Fig. 8(d). GαqQ209L activated the ARE-LUC reporter as expected. Interestingly, co-transfection with GSK3-β-Δ9 resulted in a dose-dependent inhibition of the GαqQ209L capacity to induce ARE-LUC. Taken together these results support the model presented in Fig. 8(e), in which the muscarinic M1 receptor activation induces a Gαq/PLC-β/PKC-γ axis that results in inhibition of GSK-3β and in subsequent activation of Nrf2.

Discussion

In this study, we identify a signaling pathway that starting from the muscarinic M1 receptor leads to activation of Nrf2, the transcription factor guardian of redox homeostasis, and results in up-regulation of oxidant defense genes such as HO-1. First, we found that Cch increased HO-1 protein levels in hippocampal and cerebellar granule neurons expressing the muscarinic M1 receptor. Because primary neuronal cultures represent a mixture of several cell types with a variety of acetylcholine receptors, to study M1 signaling we expressed this receptor in pheochromocytoma PC12 cells. This cell type retains many properties of neuroendocrine cells

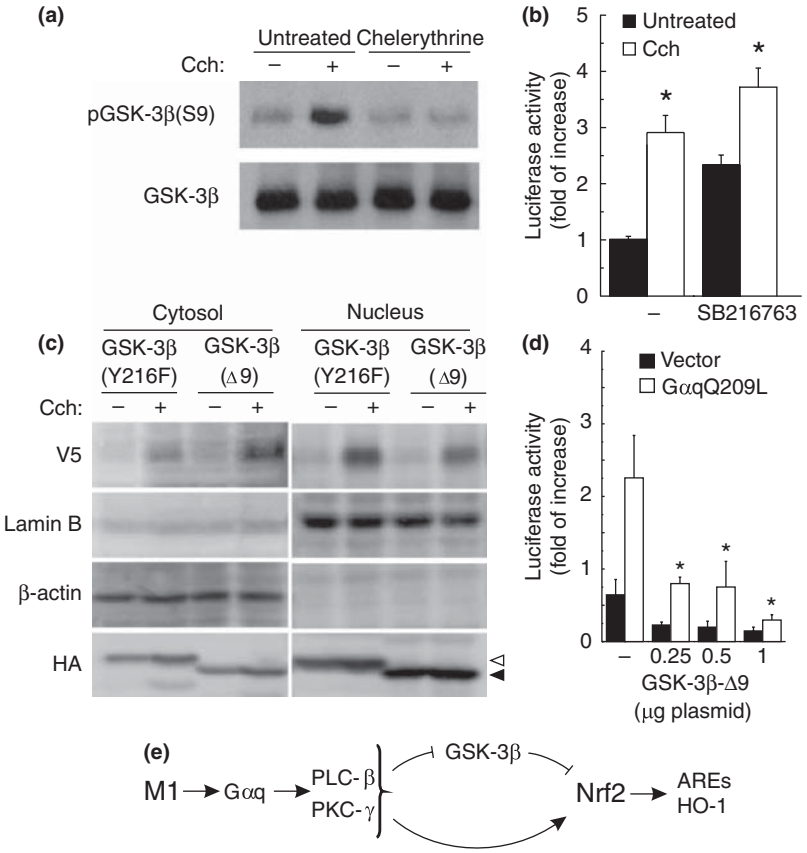

Fig. 8 Inhibition of GSK-3β by M1 signaling results in activation of AREs. (a) Phosphorylation at Ser9 of GSK-3β in response to Cch is PKC-dependent. PC12M1 cells were maintained in low-serum medium for 16 h, then pre-treated with chelerythrine for 30 min and finally stimulated with Cch for 10 min. Upper panel, immunoblot with anti-phosphoSer9-GSK-3β antibody. Lower panel, anti-GSK-3β antibody showing similar kinase amount per lane. Densitometric analysis of three similar experiments indicated a Cch-induced increase in phospho-GSK-3β(S9) of 7.2 ± 1.3 SD fold and 1.2 ± 0.4 SD fold in the absence and presence of chelerythrine respectively, after normalization for total GSK-3β levels. (b) ARE activation by Cch is increased in the presence of the GSK-3β inhibitor SB216763. PC12M1 cells were transfected with ARE-LUC (or pGL3-basic as a control) and then maintained in low-serum medium for 16 h in the presence or absence of SB216763 (10 μM) and Cch as indicated. (c) Cch-induced translocation of Nrf2 to the nucleus is decreased by GSK-3β. PC12M1 cells were co-transfected with expression vectors for V5-tagged Nrf2 and either HA-tagged, inactive mutant, GSK3β-(Y216F), as negative control, or constitutively active, HA-tagged, GSK3β-Δ9. Cells were placed in low-serum medium for 24 h and then treated with Cch (1 mM) for 30 min. Nuclear and cytosolic protein extracts were immunoblotted as indicated. Upper panel, immunoblot with anti-V5 Nrf2 antibody showing ectopically expressed Nrf2-V5. Upper middle *panel*, anti-lamin B. Lower middle panel, anti-β-actin. Lower panel, anti-HA antibody showing ectopically expressed inactive mutant HA-GSK3β-(Y216F) (empty arrow) and constitutively active mutant HA-GSK3β-(Δ9) (solid arrow). (d) Active GSK-3β mutant (GSK-3β-Δ9) blocks ARE activation by GαqQ209L in response to Cch. PC12M1 cells were co-transfected with ARE-LUC (or pGL3-basic as a control) and increasing amounts of expression vector for GSK-3β-Δ9. Cells were analyzed for luciferase activity after 24 h. Luciferase experiments were performed at least three times using 3–4 samples per group. A Student's *t*-test was used to assess differences between groups. The values in graphs correspond to the mean ± SD. Asterisk in (b) denotes statistically significant difference with $p < 0.05$ between the Cch-treated groups. Asterisks in (d) denote statistically significant differences with $p < 0.05$ between the GαqQ209L control group and each of the GαqQ209L plus GSK-3β-Δ9-transfected groups. (e) Model showing the signaling pathway identified in this study to activate Nrf2 by the M1 muscarinic receptor.

and the group of muscarinic receptors that they express has been characterized in detail (Bonisch *et al.* 1990; Michel *et al.* 1989; Berkeley and Levey 2000). Our experiments indicate that the phenotypic background of these cells is suitable to study M1 receptor signaling because in the naive un-transfected cells Cch did not elicit a significant increase in HO-1 expression (Fig. 3). On the contrary, ectopic expression of M1 resulted in a Cch-dependent increase of HO-1 protein levels. These observations designate PC12 cells as a suitable simplified system to study M1 signaling. Moreover, these observations complement previous reports initially developed by Sokolovsky's group, who analyzed the neurotrophic (Pinkas-Kramarski *et al.* 1992) and anti-apoptotic (Lindenboim *et al.* 1995) functions of M1 in M1-expressing

PC12. It is interesting that, using PC12M1 cells, Mangelus *et al.* (2001) reported an increase of ROS immediately after M1 stimulation. Further research will determine if those early produced ROS may also participate as second messengers in regulation of ARE-driven genes by disrupting the Nrf2/Keap1 interaction.

We have identified Gαq, a well-established M1-interacting Gα protein, as a crucial intermediary in M1 signaling to Nrf2. Other Gα proteins have also been reported to interact with M1 and indeed, we have found that Gα12 and Gα13 activate AREs in PC12 cells, but to a lesser extent than Gαq (data not shown). Because a preliminary study linked Gα12 and Gα13 with Nrf2 in a tumorigenic model (Cho *et al.* 2007), we focused our study on the still unexplored connection with Gαq. On the other hand, it was somewhat surprising that the Gβγ subunit did not activate AREs because previous observations with the same constructs in transformed green monkey kidney epithelial cells-7 indicated that this subunit is effective in activating PI3K/Akt (Murga *et al.* 1998) and therefore should lead to GSK-3β inhibition and Nrf2 activation. Other authors, however, have not detected this interaction in other cell models. These discrepancies may result from different signaling integration mechanisms in different cell systems.

Both pharmacologic and genetic approaches led to the conclusion that M1 and Gαq use PLC-β and classical PKCs to activate AREs. Thus, chelerythrine, a specific PKC inhibitor, and 2-APB, a blocker of store-operated calcium entry, prevented M1- and Gαq-induced activation of AREs while expression of PLC-β and PKC-γ cooperated in activation of AREs. In this study, we chose to analyze PKC-γ because this isoenzyme is abundant in brain and it co-localizes with M1 receptors in several neuronal types. Thus, we and others have observed co-localization of the M1 receptors and PKCγ in hippocampus, a brain location that is particularly sensitive to oxidative stress such as that elicited by amyloidogenic peptides or by glutamate excitotoxicity. However, we are aware that our study does not exclude the contribution of other PKCs to the regulation of AREs and the putative role of other isoenzymes, including PKC-α and PKC-β, needs to be addressed in future studies.

Our work suggests that M1 should target Nrf2 by at least two mechanisms: protein stability and nuclear localization. Regarding protein stability, the quantitatively most relevant mechanism appears to be the interaction with Keap1 (Tong *et al.* 2006; Zhang 2006; Kobayashi and Yamamoto 2005). The fact that Cch increased Nrf2 protein levels (Fig. 4d and e) and at the same time required PKC for ARE induction (Fig. 6) suggests that the observed increase in Nrf2 protein levels is mediated at least in part through PKC-mediated disruption of the Nrf2/Keap1 degradation complex. Phosphorylation of Nrf2 at Ser40 through a PKC-based mechanism has been reported to interfere with Nrf2/Keap1 leading to Nrf2 stabilization (Cho *et al.* 2007; Rushworth *et al.* 2006; Zhang and Forman 2007). However, while our results suggest a role of PKC on Nrf2 stability the specific contribution of S40 phosphorylation is not clear in our system because the S40A mutant was still effective in mediating much of M1 signaling to AREs.

Regarding subcellular localization, Nrf2 is submitted to a nuclear cytoplasmic shuttling cycle and in previous studies, we have demonstrated that GSK-3β excludes Nrf2 from the nucleus (Salazar *et al.* 2006; Rojo *et al.* 2008a). Therefore, the increased Nrf2 nuclear levels following M1-induction (Fig. 4f) together with the fact that GSK-3β counteracted this effect (Fig. 8c) suggests that nuclear Nrf2 accumulation requires GSK-3β inhibition. Several studies describe that PKCs phosphorylate GSK-3β at Ser9 leading to its inactivation (Ballou *et al.* 2001; Chen *et al.* 2000; Garrido *et al.* 2002). Some of these studies were performed with classical PKC-enriched fractions from brain (Goode *et al.* 1992) and with PKC-γ (Goode *et al.* 1992; Marais *et al.* 1990; Shin *et al.* 2002). Consistent with these reports, PKC inhibition with chelerythrine resulted in drastic reduction of phospho-Ser9-GSK-3β levels. Therefore, PKC-mediated phosphorylation of GSK-3β is a plausible mechanism to inhibit this kinase and accumulate Nrf2 in the nucleus.

Considering that M1 appears to use several pathways to activate Nrf2 is interesting to estimate the relative contribution of GSK-3β inhibition. The GSK-3β inhibitor SB216763 (and lithium, not shown) activated by itself and cooperated with Cch to induce the ARE-Luc reporter. However, the fact that ARE induction by Cch was stronger than that of SB216763 alone also suggests that Cch activates other signaling pathways that cooperate with GSK-3β inhibition. Therefore, in this system GSK-3β inhibition appears to be part but not the only mediator for whole M1-dependent activation of Nrf2. Additional mechanism involved in M1 signaling to Nrf2 need to be identified in the future and may include, apart from direct PKC-mediated dissociation of Nrf2/Keap1, a role for MAPK and PI3K/Akt pathways.

Recent evidence implicates GSK-3β in promotion of cell death and conversely inhibition of GSK-3β has been associated with survival under a variety of cytotoxic conditions that go together with oxidative stress (Balaraman *et al.* 2006; Chen *et al.* 2004; Forlenza *et al.* 2000; Lee *et al.* 2007). Regarding Alzheimer's disease, GSK-3β participates in the regulation of processes leading to Aβ deposition and neurofibrillary tangle formation. Parallel to these evidences, the use of muscarinic agonists, have been envisioned as a therapeutic option. Our study provides a new rational to design a selective M1 agonist in neurodegenerative diseases that, like Alzheimer's disease, affect cholinergic neurodegeneration. Such agonist might have a more evident antioxidant effect on the post-synaptic neurons but in addition if M1 might behave in some cholinergic neurons as an auto-receptor then M1 agonists might provide supplementary direct antioxidant benefit to the pre-synaptic neuron.

Moreover, some reaction products of Nrf2-regulated phase II enzymes are diffusible, as for instance HO-1-mediated release of carbon monoxide, and may have paracrine effects. Therefore, in addition to restoring cholinergic hypofunction at the M1 receptor level, and reducing Aβ deposition and tau pathology, our study suggests a supplementary role of cholinemimetics in protection against oxidative stress through the activation of Nrf2.

Acknowledgements

This work was supported by grant SAF2007-62646 and Sandra Espada is recipient of a FPI fellowship from the Spanish Ministry of Science and Innovation.

References

Arai K., Maruyama Y., Nishida M., Tanabe S., Takagahara S., Kozasa T., Mori Y., Nagao T. and Kurose H. (2003) Differential requirement of G alpha12, G alpha13, G alphaq, and G beta gamma for endothelin-1-induced c-Jun NH2-terminal kinase and extracellular signal-regulated kinase activation. *Mol. Pharmacol.* **63**, 478–488.

Balaraman Y., Limaye A. R., Levey A. I. and Srinivasan S. (2006) Glycogen synthase kinase 3beta and Alzheimer's disease: pathophysiological and therapeutic significance. *Cell. Mol. Life Sci.* **63**, 1226–1235.

Ballou L. M., Tian P. Y., Lin H. Y., Jiang Y. P. and Lin R. Z. (2001) Dual regulation of glycogen synthase kinase-3beta by the alpha1A-adrenergic receptor. *J. Biol. Chem.* **276**, 40910–40916.

Berkeley J. L. and Levey A. I. (2000) Muscarinic activation of mitogen-activated protein kinase in PC12 cells. *J. Neurochem.* **75**, 487–493.

Bloom D. A. and Jaiswal A. K. (2003) Phosphorylation of Nrf2 at Ser40 by protein kinase C in response to antioxidants leads to the release of Nrf2 from INrf2, but is not required for Nrf2 stabilization/accumulation in the nucleus and transcriptional activation of antioxidant response element-mediated NAD(P)H:quinone oxidoreductase-1 gene expression. *J. Biol. Chem.* **278**, 44675–44682.

Bonisch H., Boer R., Dobler M. and Schudt C. (1990) Pharmacological characterization of muscarine receptors of PC12 (rat phaeochromocytoma) cells. *Naunyn Schmiedebergs Arch. Pharmacol.* **341**, 158–164.

Butterfield D. A., Perluigi M. and Sultana R. (2006) Oxidative stress in Alzheimer's disease brain: new insights from redox proteomics. *Eur. J. Pharmacol.* **545**, 39–50.

Caccamo A., Oddo S., Billings L. M., Green K. N., Martinez-Coria H., Fisher A. and LaFerla F. M. (2006) M1 receptors play a central role in modulating AD-like pathology in transgenic mice. *Neuron* **49**, 671–682.

Chen R. H., Ding W. V. and McCormick F. (2000) Wnt signaling to beta-catenin involves two interactive components. Glycogen synthase kinase-3beta inhibition and activation of protein kinase C. *J. Biol. Chem.* **275**, 17894–17899.

Chen G., Bower K. A., Ma C., Fang S., Thiele C. J. and Luo J. (2004) Glycogen synthase kinase 3beta (GSK3beta) mediates 6-hydroxydopamine-induced neuronal death. *FASEB J.* **18**, 1162–1164.

Cho M. K., Kim W. D., Ki S. H., Hwang J. I., Choi S., Lee C. H. and Kim S. G. (2007) Role of Galpha12 and Galpha13 as novel switches for the activity of Nrf2, a key antioxidative transcription factor. *Mol. Cell. Biol.* **27**, 6195–6208.

Cuadrado A., Molloy C. J. and Pech M. (1990) Expression of protein kinase CI in NIH 3T3 cells increases its growth response to specific activators. *FEBS Lett.* **260**, 281–284.

De Vivo M., Chen J., Codina J. and Iyengar R. (1992) Enhanced phospholipase C stimulation and transformation in NIH-3T3 cells expressing Q209LGq-alpha-subunits. *J. Biol. Chem.* **267**, 18263–18266.

Delmas P., Wanaverbecq N., Abogadie F. C., Mistry M. and Brown D. A. (2002) Signaling microdomains define the specificity of receptor-mediated InsP(3) pathways in neurons. *Neuron* **34**, 209–220.

Felder C. C. (1995) Muscarinic acetylcholine receptors: signal transduction through multiple effectors. *FASEB J.* **9**, 619–625.

Felder C. C., Bymaster F. P., Ward J. and DeLapp N. (2000) Therapeutic opportunities for muscarinic receptors in the central nervous system. *J. Med. Chem.* **43**, 4333–4353.

Fisher A., Brandeis R., Bar-Ner R. H., Kliger-Spatz M., Natan N., Sonego H., Marcovitch I. and Pittel Z. (2002a) AF150(S) and AF267B: M1 muscarinic agonists as innovative therapies for Alzheimer's disease. *J. Mol. Neurosci.* **19**, 145–153.

Fisher A., Brandeis R., Haring R., Bar-Ner N., Kliger-Spatz M., Natan N., Sonego H., Marcovitch I. and Pittel Z. (2002b) Impact of muscarinic agonists for successful therapy of Alzheimer's disease. *J. Neural Transm. Suppl.* **62**, 189–202.

Fisher A., Pittel Z., Haring R., Bar-Ner N., Kliger-Spatz M., Natan N., Egozi I., Sonego H., Marcovitch I. and Brandeis R. (2003) M1 muscarinic agonists can modulate some of the hallmarks in Alzheimer's disease: implications in future therapy. *J. Mol. Neurosci.* **20**, 349–356.

Forlenza O. V., Spink J. M., Dayanandan R., Anderton B. H., Olesen O. F. and Lovestone S. (2000) Muscarinic agonists reduce tau phosphorylation in non-neuronal cells via GSK-3beta inhibition and in neurons. *J. Neural. Transm.* **107**, 1201–1212.

Garrido J. L., Godoy J. A., Alvarez A., Bronfman M. and Inestrosa N. C. (2002) Protein kinase C inhibits amyloid beta peptide neurotoxicity by acting on members of the Wnt pathway. *FASEB J.* **16**, 1982–1984.

Goode N., Hughes K., Woodgett J. R. and Parker P. J. (1992) Differential regulation of glycogen synthase kinase-3 beta by protein kinase C isotypes. *J. Biol. Chem.* **267**, 16878–16882.

Huang H. C., Nguyen T. and Pickett C. B. (2002) Phosphorylation of Nrf2 at Ser-40 by protein kinase C regulates antioxidant response element-mediated transcription. *J. Biol. Chem.* **277**, 42769–42774.

Jerusalinsky D., Kornisiuk E. and Izquierdo I. (1997) Cholinergic neurotransmission and synaptic plasticity concerning memory processing. *Neurochem. Res.* **22**, 507–515.

Katoh Y., Iida K., Kang M. I., Kobayashi A., Mizukami M., Tong K. I., McMahon M., Hayes J. D., Itoh K. and Yamamoto M. (2005) Evolutionary conserved N-terminal domain of Nrf2 is essential for the Keap1-mediated degradation of the protein by proteasome. *Arch. Biochem. Biophys.* **433**, 342–350.

Kensler T. W., Wakabayashi N. and Biswal S. (2007) Cell survival responses to environmental stresses via the Keap1-Nrf2-ARE pathway. *Annu. Rev. Pharmacol. Toxicol.* **47**, 89–116.

Kobayashi M. and Yamamoto M. (2005) Molecular mechanisms activating the Nrf2-Keap1 pathway of antioxidant gene regulation. *Antioxid. Redox Signal.* **7**, 385–394.

Kobayashi A., Ohta T. and Yamamoto M. (2004) Unique function of the Nrf2-Keap1 pathway in the inducible expression of antioxidant and detoxifying enzymes. *Methods Enzymol.* **378**, 273–286.

Koch H. J., Haas S. and Jurgens T. (2005) On the physiological relevance of muscarinic acetylcholine receptors in Alzheimer's disease. *Curr. Med. Chem.* **12**, 2915–2921.

Lee K. Y., Koh S. H., Noh M. Y., Park K. W., Lee Y. J. and Kim S. H. (2007) Glycogen synthase kinase-3beta activity plays very important roles in determining the fate of oxidative stress-inflicted neuronal cells. *Brain Res.* **1129**, 89–99.

Levey A. I., Kitt C. A., Simonds W. F., Price D. L. and Brann M. R. (1991) Identification and localization of muscarinic acetylcholine receptor proteins in brain with subtype-specific antibodies. *J. Neurosci.* **11**, 3218–3226.

Lindenboim L., Pinkas-Kramarski R., Sokolovsky M. and Stein R. (1995) Activation of muscarinic receptors inhibits apoptosis in PC12M1 cells. *J. Neurochem.* **64**, 2491–2499.

Mangelus M., Kroyter A., Galron R. and Sokolovsky M. (2001) Reactive oxygen species regulate signaling pathways induced by M1 muscarinic receptors in PC12M1 cells. *J. Neurochem.* **76**, 1701–1711.

Marais R. M., Nguyen O., Woodgett J. R. and Parker P. J. (1990) Studies on the primary sequence requirements for PKC-alpha, -beta 1 and -gamma peptide substrates. *FEBS Lett.* **277**, 151–155.

Michel A. D., Stefanich E. and Whiting R. L. (1989) PC12 phaeochromocytoma cells contain an atypical muscarinic receptor binding site. *Br. J. Pharmacol.* **97**, 914–920.

Moreira P. I., Smith M. A., Zhu X., Nunomura A., Castellani R. J. and Perry G. (2005) Oxidative stress and neurodegeneration. *Ann. NY Acad. Sci.* **1043**, 545–552.

Murga C., Laguinge L., Wetzker R., Cuadrado A. and Gutkind J. S. (1998) Activation of Akt/protein kinase B by G protein-coupled receptors. A role for alpha and beta gamma subunits of heterotrimeric G proteins acting through phosphatidylinositol-3-OH kinasegamma. *J. Biol. Chem.* **273**, 19080–19085.

Neves S. R., Ram P. T. and Iyengar R. (2002) G protein pathways. *Science* **296**, 1636–1639.

Pinkas-Kramarski R., Stein R., Lindenboim L. and Sokolovsky M. (1992) Growth factor-like effects mediated by muscarinic receptors in PC12M1 cells. *J. Neurochem.* **59**, 2158–2166.

Rojo A. I., Salinas M., Martin D., Perona R. and Cuadrado A. (2004) Regulation of Cu/Zn-superoxide dismutase expression via the phosphatidylinositol 3 kinase/Akt pathway and nuclear factor-kappaB. *J. Neurosci.* **24**, 7324–7334.

Rojo A. I., Sagarra M. R. and Cuadrado A. (2008a) GSK-3beta down-regulates the transcription factor Nrf2 after oxidant damage: relevance to exposure of neuronal cells to oxidative stress. *J. Neurochem.* **105**, 192–202.

Rojo A. I., Rada P., Egea J., Rosa A. O., Lopez M. G. and Cuadrado A. (2008b) Functional interference between glycogen synthase kinase-3 beta and the transcription factor Nrf2 in protection against kainate-induced hippocampal cell death. *Mol. Cell. Neurosci.* **39**, 125–132.

Rossi M. A., Mash D. C. and deToledo-Morrell L. (2005) Spatial memory in aged rats is related to PKCgamma-dependent G-protein coupling of the M1 receptor. *Neurobiol. Aging* **26**, 53–68.

Rushworth S. A., Ogborne R. M., Charalambos C. A. and O'Connell M. A. (2006) Role of protein kinase C delta in curcumin-induced antioxidant response element-mediated gene expression in human monocytes. *Biochem. Biophys. Res. Commun.* **341**, 1007–1016.

Salazar M., Rojo A. I., Velasco D., de Sagarra R. M. and Cuadrado A. (2006) Glycogen synthase kinase-3beta inhibits the xenobiotic and antioxidant cell response by direct phosphorylation and nuclear exclusion of the transcription factor Nrf2. *J. Biol. Chem.* **281**, 14841–14851.

Salinas M., Diaz R., Abraham N. G., Ruiz de Galarreta C. M. and Cuadrado A. (2003) Nerve growth factor protects against 6-hydroxydopamine-induced oxidative stress by increasing expression of heme oxygenase-1 in a phosphatidylinositol 3-kinase-dependent manner. *J. Biol. Chem.* **278**, 13898–13904.

Shin S. Y., Yoon S. C., Kim Y. H., Kim Y. S. and Lee Y. H. (2002) Phosphorylation of glycogen synthase kinase-3beta at serine-9 by phospholipase Cgamma1 through protein kinase C in rat 3Y1 fibroblasts. *Exp. Mol. Med.* **34**, 444–450.

Tang F. R., Lee W. L., Gao H., Chen Y., Loh Y. T. and Chia S. C. (2004) Expression of different isoforms of protein kinase C in the rat hippocampus after pilocarpine-induced status epilepticus with special reference to CA1 area and the dentate gyrus. *Hippocampus* **14**, 87–98.

Tong K. I., Kobayashi A., Katsuoka F. and Yamamoto M. (2006) Two-site substrate recognition model for the Keap1-Nrf2 system: a hinge and latch mechanism. *Biol. Chem.* **387**, 1311–1320.

Wei J., Walton E. A., Milici A. and Buccafusco J. J. (1994) m1–m5 muscarinic receptor distribution in rat CNS by RT-PCR and HPLC. *J. Neurochem.* **63**, 815–821.

Wess J. (2003) Novel insights into muscarinic acetylcholine receptor function using gene targeting technology. *Trends Pharmacol. Sci.* **24**, 414–420.

Youdim M. B. and Buccafusco J. J. (2005) CNS Targets for multi-functional drugs in the treatment of Alzheimer's and Parkinson's diseases. *J. Neural. Transm.* **112**, 519–537.

Zhang D. D. (2006) Mechanistic studies of the Nrf2-Keap1 signaling pathway. *Drug Metab. Rev.* **38**, 769–789.

Zhang H. and Forman H. J. (2007) Acrolein induces heme oxygenase-1 through PKC-{delta} and PI3K in human bronchial epithelial cells. *Am. J. Respir. Cell Mol. Biol.* **38**, 483–490.

